

Excitation Energy Transfer in the Photosystem II Core Antenna Complex CP43 Studied by Femtosecond Visible/Visible and Visible/Mid-Infrared Pump Probe Spectroscopy

Mariangela Di Donato,* Rienk van Grondelle, Ivo H. M. van Stokkum, and Marie Louise Groot

Department of Physics and Astronomy, Faculty of Sciences, Vrije Universiteit, 1081 HV Amsterdam, The Netherlands

Received: December 4, 2006; In Final Form: March 1, 2007

Excitation energy transfer in the Photosystem II core antenna complex CP43 has been investigated by vis/vis and vis/mid-IR pump–probe spectroscopy with the aim of understanding the relation between the dynamics of energy transfer and the structural arrangement of individual chlorophyll molecules within the protein. Energy transfer was found to occur on time scales of 250 fs, 2–4 ps, and 10–12 ps. The vis/mid-IR difference spectra show that the excitation is initially distributed over chlorophylls located in environments with different polarity, since two 9-keto C=O stretching bleachings, at 1691 and 1677 cm^{-1} , are observable at early delay times. Positive signals in the initial difference spectra around 1750 and 1720 cm^{-1} indicate the presence of a charge transfer state between strongly interacting chlorophylls. We conclude, both from the spectral behavior in the visible when the annihilation processes are increased and from the vis/mid-IR data, that there are two pigments (one absorbing around 670 nm and one at 683 nm) which are not connected to the other pigments on a time scale faster than 10–20 ps. Since, in the IR, on a 10 ps time scale the population of the 1691 cm^{-1} mode almost disappears, while the 1677 cm^{-1} mode is still significantly populated, we can conclude that at least some of the red absorbing pigments are located in a polar environment, possibly forming H-bonds with the surrounding protein.

Introduction

The primary processes of energy transduction and charge separation in green plants occur in two large protein–pigment complexes, Photosystem I (PSI) and Photosystem II (PSII). The PSII core contains two antenna proteins, CP43 and CP47, and the D1D2-cytb559 reaction center (RC), where charge separation occurs.¹ A 3.4 Å structure of the PSII core from cyanobacteria was published in 2004² which was recently improved to 3.0 Å.³ Structural data indicate that the CP43 core complex binds 14 chlorophylls (Chls) and 2 or 3 β -carotenes, while 17 Chls and at least 2 carotenoids have been assigned to CP47. Although the determination of the X-ray structure of the PSII core has given new insight in our understanding of energy and electron transfer processes occurring during the early photosynthetic events, the resolution at which the structure is currently available does not allow the recognition of the details of protein–pigment interactions and thus the elucidation of the energy transfer pathways inside the antennas and toward the D1D2 RC. Since both CP43 and CP47 are close to the D1D2 reaction center, it is generally believed that they have an important role in transferring the energy absorbed from the major antenna LHC II to the RC. In particular, CP43 is closely associated to the D1 polypeptide, and its position appears to be very suited to accept energy from CP26 and to transfer it to the RC, while CP47 is believed to have, besides its light-harvesting function, a more important role in the dimerization of the PSII core complex.⁴ The two core antennas are structurally related since both are composed of three pairs of trans-membrane helices and they bind more or less the same number of Chls, which are located in symmetry-related positions. However, their spectroscopic properties are significantly different, in particular at low

temperature,^{5,6} which could imply different energy transfer dynamics. A characterization of the spectroscopic properties and intra-antenna energy transfer events occurring in isolated CP43 and CP47 could be extremely useful to clarify what happens in the intact PSII core complex upon the absorption of light. The dynamics of energy transfer and charge separation in intact PSII cores has been investigated by several groups by time-resolved fluorescence and absorption spectroscopy.^{7–10} Early studies identified kinetic components of 50–80 ps which were assigned to overall energy trapping by primary charge separation.^{7,8} Recently dominant energy transfer kinetics from the antennas to the RC of ca. 1.5 ps has been proposed.¹⁰ Both pump–probe experiments and simulations of energy transfer processes in isolated CP43 and CP47 indicate that the intra-antenna energy transfer is very multiphasic, for a large part occurring on the 0.2–0.4 ps and 2–3 ps time scale followed by a slow equilibration in about 20 ps.¹¹

A careful analysis of the steady state absorption, fluorescence, linear and circular dichroism, and Stark spectra⁶ led to the conclusion that there exist two different low-energy states with different peak positions in CP43. The Q_y region of the CP43 absorption spectrum measured at 5 K shows a main band centered at 670 nm and a red band with a very distinct narrow peak at 683 nm, which, when the temperature is raised, becomes a shoulder and then disappears due to the broadening of the whole Q_y absorption. Gaussian fitting of the 5 K absorption spectrum indicates that the red-most part of the absorption spectrum can be described by a very narrow band located at 683 nm, probably due to only one Chl molecule, and a band at slightly lower frequency, whose integrated intensity accounts for a pool of 5–6 excitonically coupled Chls, thus indicating the presence of two different sets of red absorbing pigments.

This finding also agrees with fluorescence line-narrowing experiments, which showed that, upon excitation with wavelengths below 685 nm, emission from two different pools of Chls takes place⁶ and with hole-burning experiments, which have identified two quasi-degenerate low-energy states.^{12,13} Structure-based Monte Carlo simulations of the pigment–pigment exciton interactions in CP43 and CP47 showed that in CP43 excitonic interactions of the pigments on the luminal side of the protein led to a broad absorption band around 670 nm, whereas the interactions on the stromal side gave rise to a splitting of the absorption band, with maxima at 670 nm and ~684 nm.¹¹ The two fast phases of energy transfer observed at 77 K of 0.4 and 3 ps were associated with relaxation to the lowest state within the stromal side and with relaxation from the luminal to the stromal side, respectively.¹¹ The simulations could not account for the observation of the narrow, red, single Chl band (fwhm at 4 K 2.7 nm), suggesting that the cause of the red-shifted absorption is not excitonic in nature but may be caused by (interactions with) its specific environment.

Here we report the results from both vis/vis and vis/mid-IR pump probe experiments on isolated CP43, performed with the aim to relate energy transfer processes and spectroscopic properties of a particular subgroup of pigments with structural information. The analyzed region in the mid-IR, between 1600 and 1800 cm^{-1} , mainly probes the 9-keto and 10-ester chlorophyll carbonyls, which are extremely sensitive to the polarity of the protein environment, to the presence of H-bonding interactions, and to interpigment interactions. Thus, in principle, the analysis of time-resolved absorption changes in this region should allow us to determine the protein environmental properties of the different pigments. A comparison with the structure of CP43 then enables us to directly link the dynamics of energy transfer to the individual chlorophylls in the CP43 protein. For comparison we have also measured the excitation-induced absorption changes in the visible part of the spectrum, since there is no report of these dynamics at room temperature in the literature. Because of the broadening of the absorption bands at room temperature and the use of an unselective excitation wavelength (585 nm), there is no clear signature of the energy transfer processes. Therefore we have used a range of excitation energies in order to highlight the signature of energy transfer by inducing excitation annihilation processes. It is well known that high laser powers can lead to multiple excitations within a group of connected pigments, which is followed by ultrafast annihilation upon double excitation of a single pigment, causing an acceleration of the excited state decay.¹⁴ Therefore, a comparison of absorption difference spectra obtained with different excitation energies allows us to extract information on the energy transfer processes occurring within and between different pools of pigments in CP43.

Materials and Methods

CP43 samples were isolated from spinach as previously described.⁶ For vis/mid-IR experiments the sample was concentrated to an optical density (OD) of 0.65 at 670 nm for a 20 μm optical path length and suspended in 20 mM BisTris buffer (pH 6.5) in D_2O containing 20 mM NaCl, 10 mM MgCl_2 , and 0.03% β -DM; the corresponding OD at 585 nm, the wavelength of excitation, was 0.1. For vis/vis measurement the same buffer in H_2O was used. The experimental setup consisted of an integrated Ti:sapphire oscillator-regenerative amplifier laser system (Hurricane, SpectraPhysics) operating at 1 kHz and 800 nm, producing 85 fs pulses of 0.8 mJ. A portion of the 800 nm light was used to pump a non-collinear optical parametric

amplifier to produce the excitation pulses at 585 nm, which were focused on the sample with a 20 cm lens. A second part of the 800 nm light was used to pump an optical parametric generator and amplifier with a difference frequency generator (TOPAS, Light Conversion) to produce the mid-IR probe pulses, which were focused on the sample with a 6 cm lens. The probe and pump pulses were spatially overlapped in the sample. After passing the sample, the probe pulses were dispersed in a spectrograph, imaged on a 32-element MCT detector, and fed into 32 home-built integrate and hold devices that were read every shot with a National Instruments acquisition card. To ensure a fresh spot for each laser shot, the sample was moved by a home-built Lissajous scanner. The polarization of the excitation pulse was set to the magic angle (54.7°) with respect to the IR probe pulses. A phase-locked chopper operating at 500 Hz was used to ensure that with every other shot the sample was excited and that the change in transmission could be measured. The vis/vis experiments were performed with the same setup, which was extended with an arm in which white light was generated in a 2 mm sapphire plate. This probe light was focused on the sample with the same lens used to focus the excitation pulse, dispersed on a spectrograph and imaged onto one of the arrays of a double 256 element diode array (Hamamatsu S4801-256Q). The diode array was read after every shot using a 16-bit ADC (Analogue Device) and EDT CD 20 digital I/O board. The instrument response function was about 150 fs for both experiments. For the vis/vis experiment the excitation wavelength was again 585 nm, and the excitation energy was varied between 25 and 250 nJ (six different excitation energies were used, namely 25, 50, 100, 150, 200, and 250 nJ), while for the vis/mid-IR experiment an excitation energy of 100 nJ was used. The data were subjected to global analysis.¹⁵

Visible Pump/Visible Probe Results

Absorption-difference time traces at 678 nm, collected with six different excitation pulse energies ranging from 25 to 250 nJ upon excitation at 585 nm, are shown in Figure 1.

It can be clearly seen that at high excitation energies annihilation processes lead to an acceleration of the initial decay. By dividing the areas of the absorption spectrum and the absorption difference spectrum shortly after $t = 0$ and taking into account that 50% of the observed bleach is due to stimulated emission, we can calculate that at the highest excitation energy, 250 nJ, almost 25% of the chlorophylls are bleached. For each excitation energy, the time traces collected for 255 wavelengths between 610 and 740 nm have been globally analyzed, using a sequential model with increasing lifetimes. The results are shown in Figure 2.

At the lowest power, 25 nJ, two components are present, with lifetimes of 3.5 ps and 3.1 ns. The evolution-associated difference spectrum (EADS) of the first component consists of a negative band composed of the sum of bleached absorption and stimulated emission, peaking around 676 nm, which is in the middle between absorption at 670 nm and emission at 683 nm.⁶ This initial spectrum decays in 3.5 ps into the next, slightly red-shifted spectrum, whose lifetime is 3 ns, the normal excited state lifetime for Chls in proteins. An excited state absorption around 640 nm is visible in both components. The 3.5 ps component most likely represents an energy transfer plus annihilation process between blue and blue- or red-absorbing states, since excitation on the blue side is lost but red intensity is not gained. This result is similar to that of De Weerd et al., who observed blue to red energy transfer to occur with time

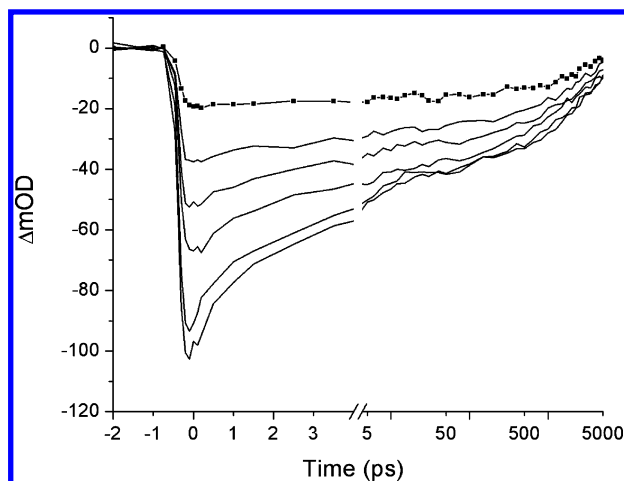


Figure 1. Time traces of CP43 taken at 678 nm as a function of the excitation power (25, 50, 100, 150, 200, 250 nJ) upon excitation at 585 nm.

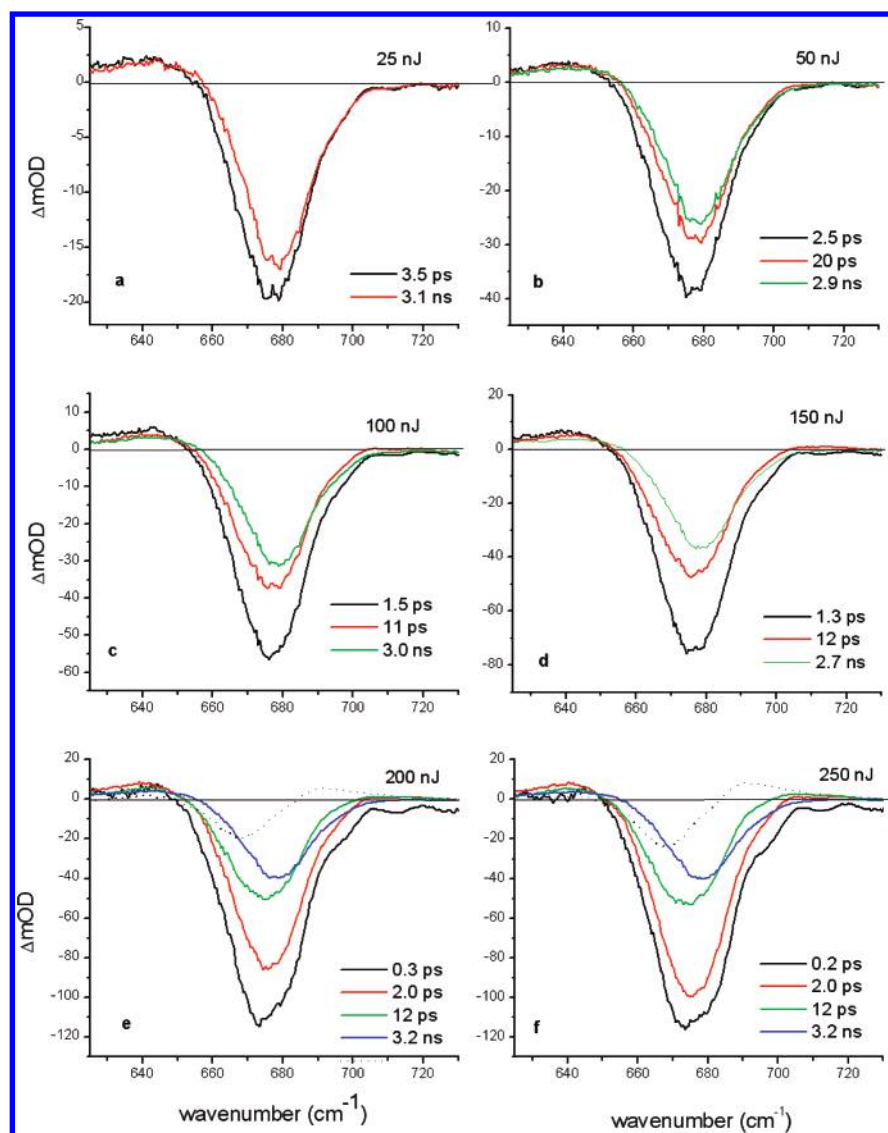


Figure 2. Evolution-associated difference spectra obtained by using a sequential model with increasing lifetimes for a data set collected with different excitation energies. Double-difference spectra between the two longest living components are shown as a dotted line in panels e and f.

constants of 0.4 and 3.4 ps at 77 K.¹¹ When the excitation energy is augmented, more complicated dynamics takes place. With 50 nJ excitation energy an additional component with a lifetime of 20 ps appears. Also in this case the short 2.5 ps lifetime component most likely represents annihilation between blue and blue/red states, but its relative amplitude has increased. The 20

ps EADS is slightly red-shifted (2 nm) and decays into the 3 ns spectrum with a small loss of intensity on the peak and blue side of the spectrum. The spectra obtained with excitation powers of 100 and 150 nJ each show similar features. The lifetime of the first component has become shorter (~ 1.5 ps) and in both cases this component now represents decay of both

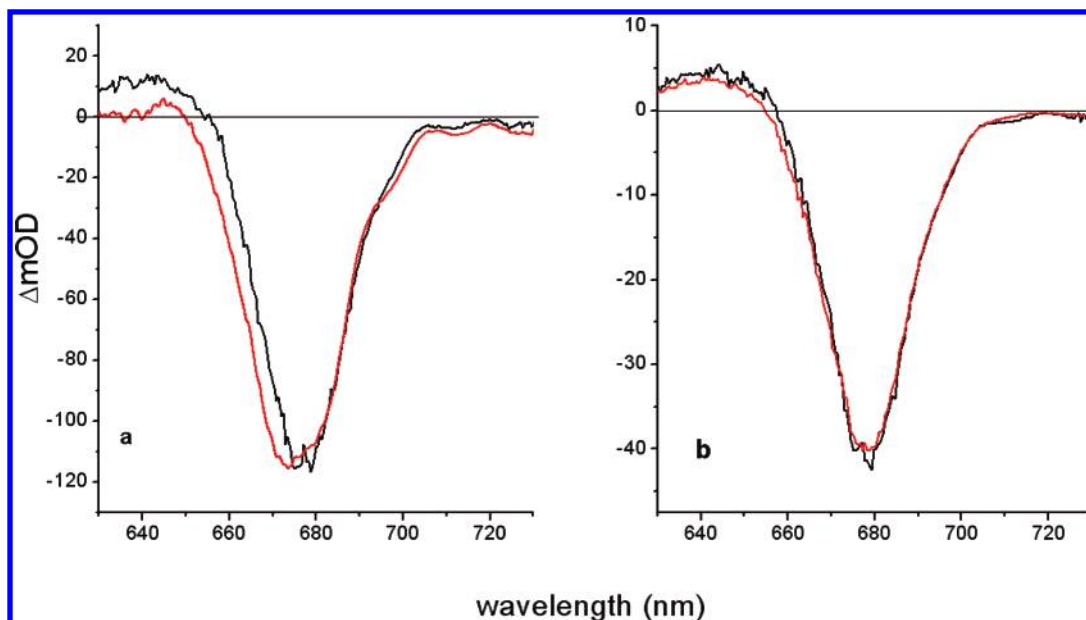


Figure 3. Comparison of (a) the first and (b) the long-living component taken respectively with 25 (black spectrum) and 250 nJ (red spectrum) excitation power.

red and blue intensity. The intermediate component (10–12 ps) shows the features of a blue to red energy transfer process, since its evolution corresponds to a loss of excitation on the blue side and a corresponding signal increase on the red side. This process is even more pronounced when the two higher excitation energies are considered. In both cases an additional ultrafast component appears (0.3–0.2 ps) which represents annihilation both between blue and blue/red states and between different red absorbing states. The following 2 ps component now mostly corresponds to a decay of red intensity, while a component with a lifetime of 12 ps is still present. As in the previous case it likely represents a blue to red energy transfer process, as is clearly shown by the decay associated difference spectra (DADS) representing the difference between this component and the long-living one, traced as a dotted line in Figure 2e,f.

The spectrum of the 12 ps component appears to be mainly conservative, which is quite unexpected if we consider that energy transfer and annihilation processes have occurred already and that a red site is likely to be populated. However, this result closely resembles what was observed in the CP47 antenna complex.¹⁶ The presence of the 12 ps conservative component indicates two facts: (1) excited blue states are still present on the 10 ps time scale and (2) an extra red state, not populated by the previous energy transfer processes, should exist. We suggest that, at high excitation density, annihilation between the bulk red states is faster than (some of the) blue to red energy transfer, leading to a relative under-population of a pool of red bulk Chls, which may result in a relatively larger difference signal than at low excitation conditions.

Also in analogy with CP47, the early time spectra, shown in Figure 3, are different, with the 250 nJ spectrum being broader and blue-shifted with respect to the 25 nJ spectrum, whereas the spectra of the long-living components obtained with high and low excitation energy do not show any difference.

The blue shift observed in the case of high excitation density can be explained by a relatively lower population of red pigments (also associated with a positive absorption increase around 660–670 nm, which possibly represents a transition of excitonic nature) due to very fast annihilation within a pool of red absorbing states within the time scale of the excitation pulse (<100 fs), in agreement with the explanation above. Finally

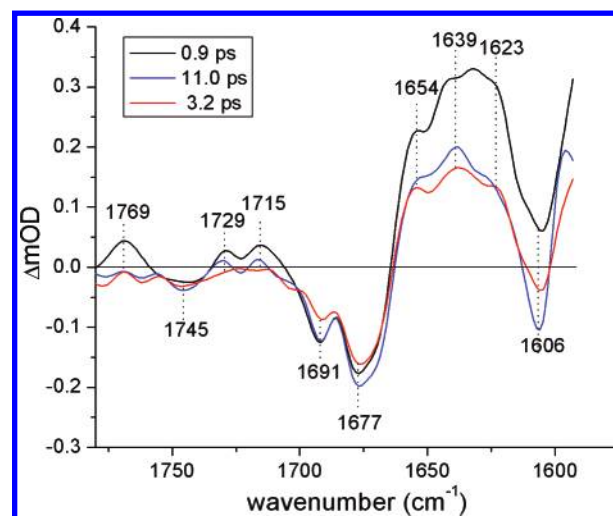


Figure 4. Evolution-associated difference spectra resulting from a global analysis with increasing lifetime for pump–probe measurements in the mid-IR region.

we note that the sub-picosecond EADS obtained with 200 or 250 nJ excitation energy are slightly blue-shifted with respect to the following 2 ps spectrum, thus representing annihilation between both blue and blue/red absorbing states. This finding is in agreement with previous modeling of time-resolved absorption data, where a 0.4 ps process has been observed after excitation at 670 nm and assigned to relaxation to a lowest state absorbing at ca. 680 nm.¹¹

Visible Pump/Mid-IR Probe Measurements

In the case of the vis/mid-IR pump probe experiment, three time components are necessary to fit the data: 0.9 ps, 11.0 ps, and 3.2 ns, in fairly good agreement with the vis/vis experiments performed with similar excitation power (100 nJ). The evolution-associated difference spectra obtained by global analysis are shown in Figure 4, while selected time traces with the fit resulting from global analysis are presented in Figure 5.

The 0.9 ps spectrum shows negative bands at 1745, 1691, 1677, and 1606 cm^{-1} , positive features at 1769, 1729, and 1715

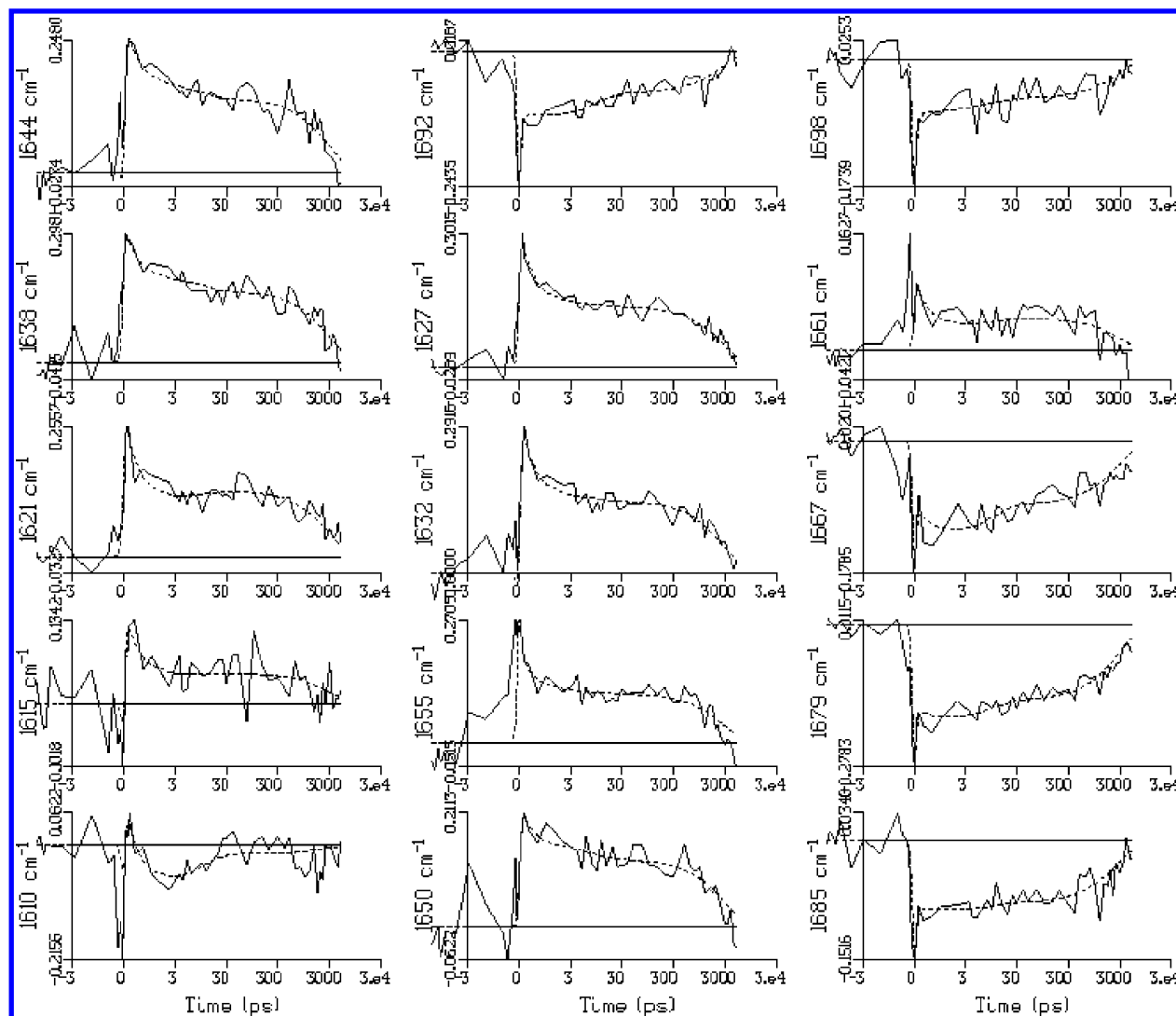


Figure 5. Selected time traces collected in the CP43 vis/mid-IR pump–probe experiment, with the fit resulting from global analysis.

cm^{-1} , and a broad absorption peaking roughly around 1640 cm^{-1} . The two bleaching bands at 1691 and 1677 cm^{-1} can be assigned to stretching modes of the 9-keto chlorophyll carbonyls, while the negative band at 1745 cm^{-1} most likely represents the bleaching of the 10-ester Chl carbonyl. The band observed at 1606 cm^{-1} has been assigned by *in vitro* FTIR measurements on Chl *a* to a ring mode sensitive to coordination number of the central Mg atom, and the observed value is indicative for penta-coordinate Chl.¹⁷ The 9-keto bands are very sensitive to their surroundings, and downshifts even higher than 20 cm^{-1} can be expected with respect to the frequency observed in nonpolar solvents (1695 cm^{-1} in THF^{18–20}) due to the presence of hydrogen bonds or different polarity of the surrounding medium. According to their frequencies, the 1691 cm^{-1} band is representative of one or more Chls having their 9-keto group in an apolar environment, without H-bonds, while the downshifted 1677 cm^{-1} band can be assigned to molecules located in a more polar environment, probably forming H-bonds. Upon excitation, the 9-keto bands are downshifted to 1620–1650 cm^{-1} in the excited state, causing a very intense and broad feature in this region,^{16,21} which possibly hides other bleaching carbonyls absorbing in the same region.

In the absorption region characteristic of the 10-ester group it is possible to identify a broad negative peak, around 1745 cm^{-1} , and positive signals at 1769, 1729, and 1715 cm^{-1} . The presence of the positive signature at 1769 cm^{-1} in the early

spectral component is quite interesting, since both the 9-keto and 10-ester bands are expected to downshift upon chlorophyll excitation, as was observed for Chl *a* in THF²¹ and CP47¹⁶ as well as upon triplet formation of Chl.²² An upshift of these bands is instead expected upon cation formation, as observed for example in the steady state light-induced FTIR difference spectrum of the primary donor both in the bacterial and PS2 reaction center^{23,24} or in the FTIR spectrum of electrochemically generated Chl⁺ species, where upshifts of ca. 20 cm^{-1} upon cation generation are measured.²⁵ The positive signatures in the 1750–1770 cm^{-1} region observed in the 0.9 ps component could be indicative of the formation of a charge transfer (CT) state between a pair of strongly interacting chlorophylls upon or shortly after excitation. In addition, the two positive signatures at 1729 and 1715 cm^{-1} are very similar to the characteristic spectral features indicating the formation of the special pair cation, P^+ , observed in light-induced FTIR and time-resolved IR spectra of D1D2 RCs,^{21,24} due to an upshift of the keto stretching in the Chl cation state. In the case of CP43 these signals can be ascribed to a combination of excited state downshift of the 10-ester bleaching band at 1745 cm^{-1} and a 9-keto upshift of one or both the bleachings at 1691 and 1677 cm^{-1} due to charge transfer state formation. Stark spectroscopy on CP43, however, did not show the formation of charge transfer states, but the unusually small Stark signals of this protein have been attributed to a high degree of excitonic coupling between

pigments with opposing oriented dipole moments.⁶ This apparent controversy may be explained by the dynamic formation of a charge transfer state upon excitation, after the initial population leaves the Franck–Condon region that is probed by Stark spectroscopy.

The following evolution into the second component shows several spectral changes: the positive band at 1769 cm^{-1} disappears almost completely, and the two positive features at 1729 and 1715 cm^{-1} significantly reduce in intensity, apparently indicating a decay of the presumed charge transfer state. The decrease of the broad positive carbonyl band at lower frequency indicates a loss of excitation in the sample due to annihilation processes occurring on this time scale. In the carbonyl bleaching region we do not observe any change on the 1691 cm^{-1} bleaching, while at 1677 cm^{-1} there is an apparent gain of bleaching and a broadening of the signal. As already observed in the case of CP47¹⁶ the loss of excitation does not correspond to a recovery of the carbonyl bleaching, probably because the decay of the relatively more intense keto excited state band at low frequencies obscures a direct observation of the early dynamics of the bleached keto bands in the 1680 – 1670 cm^{-1} region. After 11 ps, however, both the 1691 and 1677 cm^{-1} bands decay in intensity, with the 1691 cm^{-1} signal decaying to a much larger extent. This observation indicates that on a time scale of ~ 11 ps energy transfer occurs from one or more pigments located in a nonpolar environment toward pigment(s) located in a more polar one. The occurrence of an energy transfer process on the same time scale is also observed in the vis/vis spectra.

In summary, vis/mid-IR spectra allow us to distinguish two bleaching signals, each corresponding to one or possibly more Chls located in environments with different polarity, even though the excitation wavelength used in the experiment was not frequency selective. Then, in almost 1 ps, excitations annihilate and an apparent gain of bleaching in the $\sim 1680\text{ cm}^{-1}$ region appears, possibly related to the sharpening and decay of the broad excited state band, which can partly hide negative signals in the early time component. Finally, in about 11 ps the 1691 cm^{-1} bleaching significantly recovers, while on this time scale excitations are still present on Chls localized in a more polar environment, as shown by the intensity of the 1677 cm^{-1} bleaching, which decreases only to a minor extent. This observation is in line with the occurrence of a blue to red energy transfer on a ~ 10 – 20 ps time scale, as also observed in vis/vis pump–probe measurement. The additional information which can be extracted by femto-IR measurements is that the blue pigment(s) involved in this process are located in a nonpolar environment, while the red pigment(s) toward which the energy is transferred reside in a more polar region of the protein.

Discussion

Both vis/vis and vis/mid-IR experiments show that in CP43 the excitation is initially distributed over pools of Chls with different absorption properties and that both rapid and relatively slower energy transfer and annihilation processes between molecules contained in different pools occur. Since the excitation wavelength used in all the experiments, 585 nm, is nonselective, preferential excitation is not expected, and it can be assumed that pigments both with more blue or red absorption properties will be populated, at late times, according to a Boltzmann distribution. By performing vis/vis pump–probe measurements using different excitation energies, which induced different amounts of annihilation, it was possible to highlight a relatively slow kinetic phase, showing the features of a blue to red energy

transfer process, which becomes observable when the excitation energy is raised. The same kinetic phase is also observed in the vis/mid-IR pump–probe spectra. Besides this relatively slow component, both vis/vis and vis/mid-IR data show a fast dynamic phase, consisting both of annihilation and blue to red energy transfer occurring between the initially populated pigments, which is complete in about 2 ps, for all the excitation energies. Judging from the evolution of the IR spectra, it appears that the loss of excitation taking place in the first few picoseconds also involves the decay of the early generated charge transfer state, since the positive signals at 1769 , 1729 , and 1715 cm^{-1} , which we interpreted as arising from the formation of a CT state between a pair of strongly interacting chlorophylls, largely disappear on the 1 ps time scale. If we assign the rapid decay of the CT state as being due to fast energy transfer, then this implies that its energy is not significantly lower than that of the equilibrated pool of pigments and that it has a significant transition dipole moment. Short-lived charge transfer states have been observed in several cases, mostly for systems containing transition metals. Recently very fast decay of a sub-picosecond generated charge transfer state has been reported for a supramolecular donor–bridge–acceptor system, containing a porphyrin ring covalently linked to a ruthenium complex, studied in order to produce artificial photosynthetic devices.²⁶ In the case of this system several models for the observed rapid decay of the early generated CT state have been discussed, among which was the possibility of an ultrafast equilibration between charge transfer and excited states, which could also apply to the case of CP43.

On a slower time scale, the observation of a blue to red energy transfer process occurring in ~ 10 – 20 ps points to the existence of a red state which is initially not populated, and it implies that population on a blue state is still present on this time scale. From the amplitude of the ~ 10 – 20 ps component we estimate that the process taking place on this time scale only involves a limited number of pigments, possibly only one blue and one red chlorophyll, which could thus be located in a rather isolated position in the protein structure. The infrared signatures of the isolated pigments should correspond to the two bleaching signals observed at 1691 and 1677 cm^{-1} in the mid-IR spectrum, since these features show the same dynamic evolution observed in the visible. The 1677 cm^{-1} signal is quite broad and could be initially due to more than one chlorophyll, but since it is still clearly observable in the last spectral component it has to be a characteristic marker of the red trap toward which the energy is finally transferred, while the 1691 cm^{-1} band, which decays almost completely in ~ 11 ps, can be assigned to one or a few blue pigments that transfer energy to the red trap on this time scale.

This ‘slow transfer’ phase is not observed when low excitation energy is used, both in the present work and in a previous study of time-resolved absorption spectroscopy on CP43.¹¹ This apparent contradiction can be explained by considering that at high excitation energy a relative under-population of red states is achieved by annihilation on the time scale of the exciting pulse. Both this and previous works^{6,11–13} suggested the presence of different red states in CP43. In particular, the analysis of hole burning and CD spectra showed that CP43 possesses two quasi-degenerate red states, indicated as A and B,^{12,13} whose peak maxima have been found to be almost identical (respectively 683.3 and 683.0 nm). The B state has been identified as the one responsible for the sharp feature observable in the absorption spectrum at low temperature, localized on one Chl and weakly coupled to other Chls, while the A-state is

significantly broader, and possibly excitonically coupled to other Chls.¹³ In absence of annihilation, which determines a fast loss of excitation from the excitonically coupled red states, energy transfer to the unconnected red site may not be visible because it determines very small spectral changes. Therefore, although a 10–20 ps energy transfer process is not observed using low excitation power (see also ref 11), its presence at higher excitation energies shows that there are not one but two slowly connected sites in the complex, one having more blue absorption and the other having a red absorption. The latter can be identified with the single narrow band in the absorption spectrum at low temperature⁶ which is the B-state described in refs 12 and 13, located on a single isolated Chl. Monte Carlo simulations of the excitonic interactions and energy transfer dynamics in CP43 reproduced the absorption spectrum of CP43, with the exception of the narrow red-most absorption band. It was therefore suggested that the origin of this band was environmental rather than excitonic. In the calculation, the Q_y transitions of all pigments were taken in the plane of the membrane, which resulted in a fairly good reproduction of the ultrafast relaxation times—those faster than 3 ps.¹¹ Analysis of time-resolved vis/mid-IR data reported in this work suggests that the 9-keto carbonyl of the isolated Chl absorbs at 1677 cm^{-1} , and it is thus located in a polar environment, possibly forming a quite strong H-bond with the surrounding residues. This finding is in agreement with the non-excitonic red shift of its absorption.

In order to support the arguments presented in this discussion, a spectral model has been applied to time-resolved vis-pump/vis-probe data on CP43. The interested reader can find the results of this modeling in the Supporting Information of this paper, where the results of an analogous analysis applied to the previously published data on CP47¹⁶ are also reported.

Finally, to gain more insight in where the isolated pigments are located, we now will link our spectroscopic observations with the current structural information obtainable from the available crystal structure. We emphasize, however, that the X-ray data are only available for cyanobacteria and that there could be some differences with spinach. Moreover, although the crystal structure is now solved with sufficient accuracy, some details of the pigment protein interactions, such as the presence of H-bonds, can only be hypothesized at the moment since hydrogen positions are still not resolved and uncertainty about the position of some heavy atoms and the orientation of side chains still remains. The analysis of the crystal structure of the cyanobacterium *T. elongatus*^{2,3} shows that all the Chl pigments associated to CP43 are arranged in two layers near the stromal and luminal side of the membrane, except for one Chl (Chl46, Loll numeration), which is located between the two layers. There are five pairs of Chls with a center-to-center distance less than 10 Å, mostly localized on the stromal side. Among them Chl45 and Chl46 have pair interactions with two other Chls: Chl45 is at 8.6 Å from Chl44 (center-to-center distance) and at 9.7 Å from Chl46, which also interacts with Chl34, at a distance of 9.9 Å. Both Chl45 and Chl46 do not appear to have any polar residue in the surrounding area of their 9-keto and 10-ester groups, while Chl34 shows possible H-bonding interactions with a tyrosine and a histidine residues. There have been some suggestions in the literature about the possible location of red states in CP43. For instance, theoretical studies relating the structural properties and the energy transfer efficiency inside the antennas and toward the reaction center in PSII^{27,28} indicated that both in CP43 and CP47 there is a unique Chl—Chl41 in CP43—which plays the most important role in transferring energy to the RC. This molecule is located on the stromal side,

is one of the nearest to the RC, and has some polar residues in its environment, but none of them appears to be suited to form a quite strong H-bond. On the same side of the membrane there is, however, another Chl—Chl47—whose 9-keto carbonyl is at H-bond distance from the side chain of an aspartic residue. This Chl also has another peculiarity, since its central Mg is not coordinated by a histidine residue, as it is for the majority of the pigments linked to CP43, but by an asparagine. Interestingly it has been suggested that the coordination by an asparagine residue is responsible for the red-shifted absorption of specific pigments contained in the antenna system of photosystem I.²⁹ This molecule, however, is not isolated, having at least three neighbor pigments, so it could possibly be part of an extended red pool of pigments which is initially populated. A more isolated pair of pigments seems to be that formed by Chl48 and Chl49, whose center-to-center distance is ~ 9.5 Å, and which are located relatively far apart from the rest of pigments linked to the stromal side of the protein. Chl48 has no possible H-bond donor in its surroundings, while the 9-keto carbonyl of Chl49 is at H-bond distance from a tyrosine residue, which makes it possible for it to absorb at 1677 cm^{-1} in the IR.

On the luminal side, the nearest Chl to the RC is Chl37, which appears to be located in a quite isolated position and is surrounded by several polar residues since at least one tryptophan and two serine residues are in a sphere of 5.0 Å around it. Furthermore, Chl37 also presents a special Mg coordination, possibly to a methionine residue, which appears however not perfectly oriented, or alternatively to a water molecule. A similarly coordinated Chl also exists in CP47, suggesting that they may also have a special role in the energy transfer process toward the RC.^{30,31} At least two of the Chls identified here by looking at the crystal structure could represent the isolated blue and red absorbing pigments, but an exact assignment requires further characterization, possibly involving the recourse to site specific mutations.

Conclusions

Combining the results of time-resolved vis/vis and vis/mid-IR pump-probe data, we have shown that energy transfer between pigments associated to CP43 has a fast component, possibly involving the formation of a charge transfer state between a pair of strongly interacting Chls and a slower one. This fast component occurs on a time scale of 10–20 ps, showing the features of a blue to red energy transfer, which becomes observable under strong annihilation conditions. We conclude from the spectral behavior that, when the annihilation processes are increased, there are two pigments (one absorbing around 670 nm and one at 683 nm) that are not connected to the other pigments on a time scale faster than 10–20 ps. The recourse to femtosecond mid-IR allowed us to show that the slower phase of energy transfer occurs between pigments located in environments with different polarity and that the red pigment is located in a polar environment, probably forming a quite strong H-bond with the surrounding residues. Linking spectroscopic information to structural data as obtained from the analysis of the 3.0 Å resolution crystal structure, we suggested plausible locations for the two ‘slow-connected’ pigments of CP43.

Acknowledgment. This work was supported by The Netherlands Organization for Scientific Research, NWO-ALW. We thank Henny van Roon for the preparation of the sample.

Supporting Information Available: Spectral model analysis of the vis/vis pump probe absorption spectra reported in this

work and of the previously published vis/vis pump–probe absorption spectra on CP47.¹⁶ This material is available via the Internet free of charge at <http://pubs.acs.org>.

References and Notes

- (1) van Grondelle, R.; Dekker, J. P.; Gillbro, T.; Sundstrom, V. *Biochim. Biophys. Acta* **1994**, *1187*, 1–65.
- (2) Ferreira, K. N.; Iverson, T. M.; Maghlaoui, K.; Barber, J.; Iwata, S. *Science* **2004**, *303*, 1831–1838.
- (3) Loll, B.; Kern, J.; Saenger, W.; Zouni, A.; Biesiadka, J. *Nature* **2005**, *438*, 1040–1044.
- (4) Eijkelhoff, C.; Dekker, J. P.; Boekema, E. J. *Biochim. Biophys. Acta* **1997**, *1321*, 10–20.
- (5) Groot, M. L.; Peterman, E. J.; van Stokkum, I. H.; Dekker, J. P.; van Grondelle, R. *Biophys. J.* **1995**, *68*, 281–290.
- (6) Groot, M.-L.; Frese, R. N.; de Weerd, F. L.; Bromek, K.; Pettersson, A.; Peterman, E. J. G.; van Stokkum, I. H. M.; van Grondelle, R.; Dekker, J. P. *Biophys. J.* **1999**, *77*, 3328–3340.
- (7) Schatz, G. H.; Brock, H.; Holzwarth, A. R. *Biophys. J.* **1988**, *54*, 397–405.
- (8) Barter, L. M. C.; Bianchetti, M.; Jeans, C.; Schilstra, M. J.; Hankamer, B.; Diner, B. A.; Barber, J.; Durrant, J. R.; Klug, D. R. *Biochemistry* **2001**, *40*, 4026–4034.
- (9) Dekker, J. P.; van Grondelle, R. *Photosynth. Res.* **2000**, *63*, 195–208.
- (10) Holzwarth, A. R.; Muller, M. G.; Reus, M.; Nowaczyk, M.; Sander, J.; Rogner, M. *Proc. Natl. Acad. Sci.* **2006**, *103*, 6895–6900.
- (11) de Weerd, F. L.; van Stokkum, I. H. M.; van Amerongen, H.; Dekker, J. P.; van Grondelle, R. *Biophys. J.* **2002**, *82*, 1586–1597.
- (12) Jankowiak, R.; Zazubovich, V.; Ratsep, M.; Matsuzaki, S.; Alfonso, M.; Picorel, R.; Seibert, M.; Small, G. J. *J. Phys. Chem. B* **2000**, *104*, 11805–11815.
- (13) Hughes, J. L.; Picorel, R.; Seibert, M.; Krausz, E. *Biochemistry* **2006**, *45*, 12345–12357.
- (14) Nuijs, A. M.; van Grondelle, R.; Joppe, H. L. P.; van Bochove, A. C.; Duysens, L. N. M. *Biochim. Biophys. Acta* **1985**, *810*, 94–105.
- (15) van Stokkum, I. H. M.; Larsen, D. S.; van Grondelle, R. *Biochim. Biophys. Acta* **2004**, *1657*, 82–104.
- (16) Groot, M. L.; Breton, J.; van Wilderen, L. J. G. W.; Dekker, J. P.; van Grondelle, R. *J. Phys. Chem. B* **2004**, *108*, 8001–8006.
- (17) Fujiwara, M.; Tasumi, M. *J. Phys. Chem.* **1986**, *90*, 250–255.
- (18) Katz, J. J.; Closs, G. L.; Pennington, F. C.; Thomas, M. R.; Strain, H. H. *J. Am. Chem. Soc.* **1963**, *85*, 3801–3809.
- (19) Feiler, U.; Mattioli, T. A.; Katheder, I.; Scheer, H.; Lutz, M.; Robert, B. *J. Raman Spectrosc.* **1994**, *25*, 365–370.
- (20) Pascal, A. A.; Caron, L.; Rousseau, B.; Lapouge, K.; Duval, J.-C.; Robert, B. *Biochemistry* **1998**, *37*, 2450–2457.
- (21) Groot, M. L.; Pawlowicz, N. P.; van Wilderen, L. J. G. W.; Breton, J.; van Stokkum, I. H. M.; van Grondelle, R. *Proc. Natl. Acad. Sci.* **2005**, *102*, 13087–13092.
- (22) Noguchi, T.; Inoue, Y.; Satoh, K. *Biochemistry* **1993**, *32*, 7186–7195.
- (23) Mantale, W.; Navedryk, E.; Tavitian, B. A.; Kreutz, W.; Breton, J. *FEBS Lett.* **1985**, *187*, 227–232.
- (24) Noguchi, T.; Tomo, T.; Inoue, Y. *Biochemistry* **1998**, *37*, 13614–13625.
- (25) Mantale, W. G.; Wollenweber, A. M.; Navedryk, E.; Breton, J. *Proc. Natl. Acad. Sci.* **1988**, *85*, 8468–8472.
- (26) Gabrielsson, A.; Hartl, F.; Zhang, H.; LindsaySmith, J. R.; Towrie, M.; Vlcek, A.; Perutz, R. N. *J. Am. Chem. Soc.* **2006**, *128*, 4253–4266.
- (27) Vasil'ev, S.; Bruce, D. *Plant Cell* **2004**, *16*, 3059–3068.
- (28) Saito, K.; Kikuchi, T.; Nakayama, M.; Mukai, K.; Sumi, H. *J. Photochem. Photobiol., A* **2005**, *86*, 175–184.
- (29) Morosinotto, T.; Breton, J.; Bassi, R.; Croce, R. *J. Biol. Chem.* **2003**, *278*, 49223–49229.
- (30) Loll, B.; Kern, J.; Zouni, A.; Saenger, W.; Biesiadka, J.; Irrgang, K.-D. *Photosynth. Res.* **2005**, *86*, 175–184.
- (31) Murray, J. W.; Duncan, J.; Barber, J. *Trends Plant Sci.* **2006**, *11*, 152–158.